Electrochemical deposition of copper oxide nanowires for photoelectrochemical applications

Le Chen,* Sudhakar Shet, Houwen Tang, Heli Wang, Todd Deutsch, Yanfa Yan,* John Turner and Mowafak Al-Jassim

Received 27th April 2010, Accepted 27th May 2010
DOI: 10.1039/c0jm01228a

We report a two-step electrochemical process to grow copper oxide nanowires without the use of templates and surfactants. The first step is to electrochemically corrode amorphous Cu–W oxides pre-sputtered on fluorine-doped tin oxide (FTO) coated glass substrates under positive potentials. The second step is to use the corroded samples to grow copper oxide nanowires electrochemically under negative potentials. We find that copper oxide nanowires grown by this method exhibit excellent contact with the FTO-coated substrates leading to good charge transfer. The oxidation states, *i.e.*, CuO or Cu_2O, and morphology of nanowires can be controlled by the applied potentials. Cu_2O nanowires grown using this method reveal moderate photoelectrochemical response and stability under illumination and under cathodic bias.

I. Introduction

In recent years, copper-oxide-based materials have found applications in various areas including heterogeneous catalysis,[1,2] gas sensing,[3] superconducting,[4] and solar energy conversion.[5–7] Copper oxides have been studied for photoelectrochemical (PEC) hydrogen production from solar-driven water splitting because they are abundant, nontoxic, and natively p-type and absorb visible light, although they face challenging issues such as instability in aqueous phases. CuO has a bandgap of ~1.2–1.5 eV[8] and Cu_2O has a bandgap of ~2.17 eV.[9] Copper oxides can be synthesized by various methods such as sputtering,[10,11] thermal evaporation,[12,13] sonochemical methods,[14] thermal relaxation,[15] and electrodeposition.[16–21] Among these methods, electrochemical deposition exhibits two major advantages: (1) it is a low-temperature growth process and can be highly cost effective; (2) it provides controlled growth, which leads to preferred morphology, structure, and orientation that fit specific applications. For PEC applications, nanostructures such as nanoparticles and nanowires are often used as an approach to enhance PEC performance due to the greatly increased surface areas. We have shown that aligned ZnO nanorods and nanocoral structures do improve PEC performance as compared to compact ZnO films grown under similar conditions.[22,23] However, it has been a challenge to grow copper oxide nanostructures on bare substrates. Typically, the growth of nanowires requires the use of a template and surfactants.

In this paper, we report a two-step electrochemical process to grow copper oxide nanowires without the use of templated substrates and surfactants. The first step is to corrode amorphous Cu–W oxides, which is pre-sputtered on fluorine-doped tin oxide (FTO)-coated glass substrates, electrochemically under positive potentials. The second step is to use the corroded samples to grow copper oxide nanowires electrochemically under negative potentials. We find that in the first step, W is corroded much faster than Cu. The remaining Cu-rich materials provide effective nucleation sites for growing copper oxide nanowires, but also provide good contact between the nanowires and FTO layer, which are beneficial for photo-generated charge-carrier collection. The oxidation states, *i.e.*, CuO or Cu_2O, and morphology of nanowires can be controlled by the applied potentials. Cu_2O nanowires grown using this method at a potential of −0.4 V reveal optimal photocurrents. Our results suggest that this two-step growth process is a unique method for growing nanostructured metal oxide semiconductors and the PEC properties of these nanostructured oxides are compared and studied in this paper.

National Renewable Energy Laboratory, Golden, CO, 80401, USA. E-mail: Le.Chen@nrel.gov; Yanfa.Yan@nrel.gov

II. Experiments

The amorphous Cu–W oxide films were deposited by reactive co-sputtering of metallic Cu and W targets. F-doped SnO_2 (FTO) (20–23 Ω cm^{-1}) coated transparent glass was used as the substrate. The distance between the targets and substrate was 8 cm. The base pressure was below 1.3×10^{-4} Pa, and the working pressure for all syntheses was 1.3 Pa, which was controlled by a throttle valve and measured with a Baratron® capacitance manometer. Argon was used as the sputtering gas and oxygen was added as the reactive gas. The mass flow rate ratio of $O_2/(O_2 + Ar)$ was 2.5/7. The substrates were kept at low temperature below 100 °C during the sputtering to avoid crystallization. The film thickness for all samples was controlled to about 1 μm as measured by stylus profilometry. The atomic ratio of Cu to W was about 1 : 1.2. More details of the deposition conditions can be found elsewhere.[24]

A three-electrode system was used for electrochemical corrosion and deposition. The copper tungsten oxide on FTO glass substrates (active area: 0.25 cm^2) served as the working electrode. A Pt sheet (area: 10 cm^2) and a Ag/AgCl electrode (with saturated KCl) were used as counter and reference electrodes, respectively. Based on the literature,[20,21] we used an electrolytic bath solution containing 3M lactic acid ($CH_3CHOHCOOH$) and 0.4M $CuSO_4$, which provided an extra copper source. The pH value of the

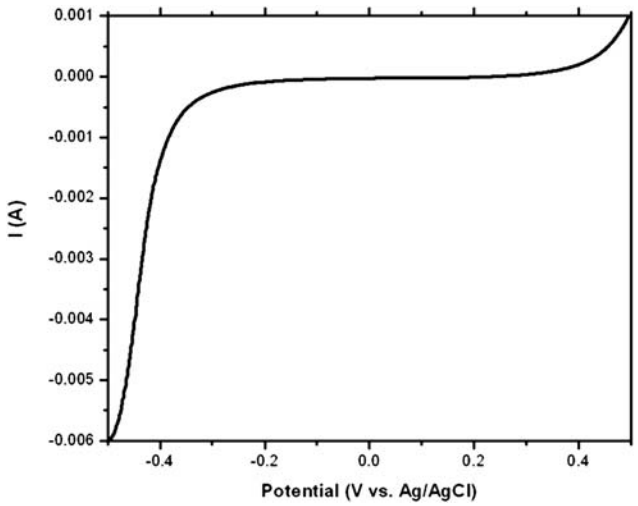

Fig. 1 A typical current–voltage curve during the linear sweeps of potential scan for the corrosion process.

solution was adjusted to 11 by adding NaOH. The corrosion, *i.e.*, the first step of our process, was carried out by applying three linear sweeps of potential scan over the amorphous copper tungsten oxide films at 3 mV s^{-1} in pure pH 11 NaOH from −0.5 V to 0.5 V, with respect to the Ag/AgCl reference electrode. A typical current–voltage curve for the linear sweeps of potential scan is shown in Fig. 1. High anodic currents at high positive potential were used to monitor the corrosion. We have also tried to conduct the corrosion at the potential corresponding to high corrosion rate, but we found that it was very difficult to control the corrosion to obtain the required morphology. The deposition bias was fixed as −0.3, −0.4 and −0.5 V *vs.* Ag/AgCl, respectively. All depositions were performed by holding the potential constant for about 2 h. The corrosion and deposition were carried out at room temperature. PEC performance of the grown materials was characterized using the same three-electrode system in a pH 11 NaOH electrolyte solution. A fiber-optic illuminator tungsten–halogen lamp with light intensity of 125 mW cm^{-2} was used as the light source. The PEC response under chopped illumination was measured during a potential sweep at a scan rate of 5 mV s^{-1}. The other details of the experiment can be found in our previous work.[23,25]

The structural and crystallinity of the grown samples were characterized by X-ray diffraction (XRD) measurements, using an X-ray diffractometer (XGEN-4000, SCINTAG, Inc.) operated with a Cu Kα radiation source at 45 kV and 37 mA. The surface morphology was observed by scanning electron microscopy (SEM, FEI Nova 630), and elemental composition was determined by energy-dispersive X-ray spectroscopy (EDX) installed on an SEM. The microstructure and Cu oxidation states were investigated by transmission electron microscopy (TEM, FEI Tecnai F20-UT) and electron energy-loss spectroscopy (EELS).

III. Results and discussion

The morphology of the amorphous Cu–W oxide film before and after corrosion has been examined by SEM, shown in Fig. 2. The

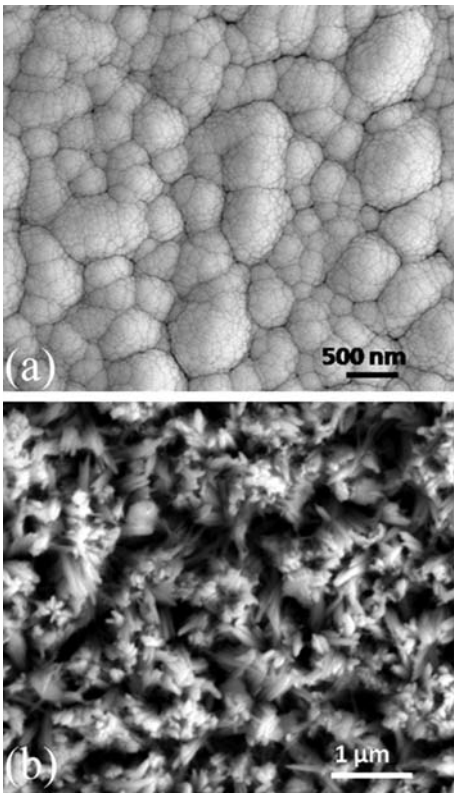

Fig. 2 SEM images of (a) as-sputtered amorphous Cu–W oxide film and (b) the same film after corrosion.

as-sputtered amorphous Cu–W oxide film exhibits a densely bundled grain structure [Fig. 2(a)]. Each grain bundle (from 200 to 400 nm in diameter) contains smaller columns with various sizes from 30 to 100 nm in diameter. However, after applying three linear sweeps of potential scan up to 0.5 V, the morphology of the thin film became very rough and the grain structure changed completely to a more porous structure [Fig. 2(b)]. EDX analysis indicated no detectable W left in the film. We found that the corrosion-induced formation of the porous structure is crucial for successful growth of copper oxide nanowires without templates or surfactants. We were unable to grow copper oxide nanowires directly on bare FTO-coated glass substrates and uncorroded amorphous Cu–W oxide films under the same growth conditions. SEM images suggest that the porous structure of copper oxide promotes the nucleation of copper oxide nanowires.

It is known that the oxidation states of copper oxide, *i.e.*, Cu, Cu_2O, or CuO, deposited by electrochemical methods are usually determined by the applied potentials and electrolyte pH value. At a fixed electrolyte pH, a high positive potential leads to a high Cu ionized state. Thus, at positive potentials, Cu and W will be dissolved from the amorphous Cu–W oxide and at negative potentials, Cu, Cu_2O, or CuO could be deposited on substrates. A more negative potential favors the formation of metallic Cu, a moderate negative potential would favor the formation of Cu_2O, and the least negative potential should favor the formation of CuO. Thus, we have applied three different potentials, −0.5 V, −0.4 V, and −0.3 V, to grow copper oxide nanowires after the first step. These samples grown by the two-step process

are labeled as CuWO-two-step-0.5V, CuWO-two-step-0.4V, and CuWO-two-step-0.3V.

Fig. 3 shows SEM images obtained from the samples electrochemically deposited at potentials of −0.3 V, −0.4 V, and −0.5 V for 2 h. Copper oxide nanowires are clearly seen. It is interesting to note a common feature in all the samples: the nanowires appear to emanate from common nucleation sites. This feature provides direct evidence that the nanowires grew radially from specific nucleation sites that were created during the first step. It is possible that the sharp tips of the corroded films enhance the electrical field and promote the nucleation and growth and inhibit the nucleation and growth on neighboring sites. These nucleation sites serve as an excellent connection between the nanowires and FTO layer, which ensures good charge transfer. However, obvious differences are also observed among these samples. The sample deposited at a potential of −0.3 V [Fig. 3(a)] has the lowest density of copper oxide nanowires as compared to the other two samples: only a small fraction of the sample is covered by copper nanowires. The nanowires in the sample deposited at potential of −0.5 V [Fig. 3(c)] have the largest sizes, both in radius and length. The size difference may be attributed to the different growth rate at different potentials. The more negative potential would lead to higher current density, which is proportional to growth rate. In addition, copper oxides in forms different from nanowires are also seen. The areas underneath the coverage of nanowire bundles indicated by the red arrows have cubic features. According to the measurement, at the end of 2 h of deposition, −621 coulombs/cm^2 were passed under a potential of −0.5 V, −488 coulombs/cm^2 were passed under a potential of −0.4 V and −334 coulombs/cm^2 were passed under a potential of −0.3 V. As the potential moved negatively, more current was passed, and the observed fraction of nanowires also increased.

We find that the presence of W in the amorphous Cu–W oxide films is critical for growing copper oxide nanowires. We have tried the two-step process on pre-sputtered CuO film. However, only cube-like films were deposited. Fig. 4(a) and 4(b) show the SEM images of the surface morphology of an as-sputtered CuO thin film and the surface of the sample after the two-step growth process at a potential of −0.4 V using CuO as the starting material. It is seen that without W in the starting material, the two-step growth process produces clusters of Cu_2O cubes instead of nanowires. From our detailed corrosion test,[24] we know that the dissolution of W is much faster than that of Cu from the amorphous Cu–W oxide films, resulting in the selective dissolution of W. The different corrosion rates could be the reason why

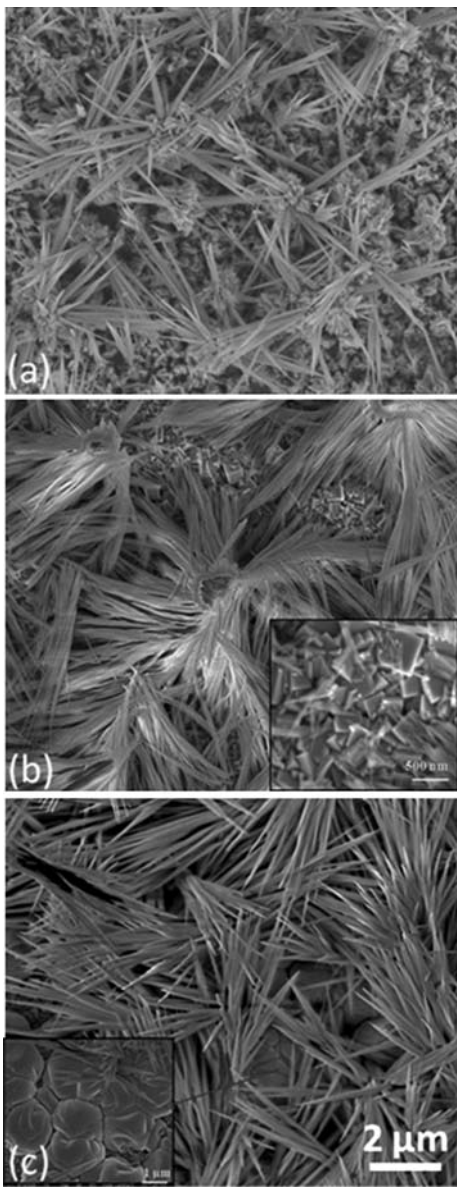

Fig. 3 SEM images of samples deposited at potentials of (a) −0.3 V, (b) −0.4 V, and (c) −0.5 V.

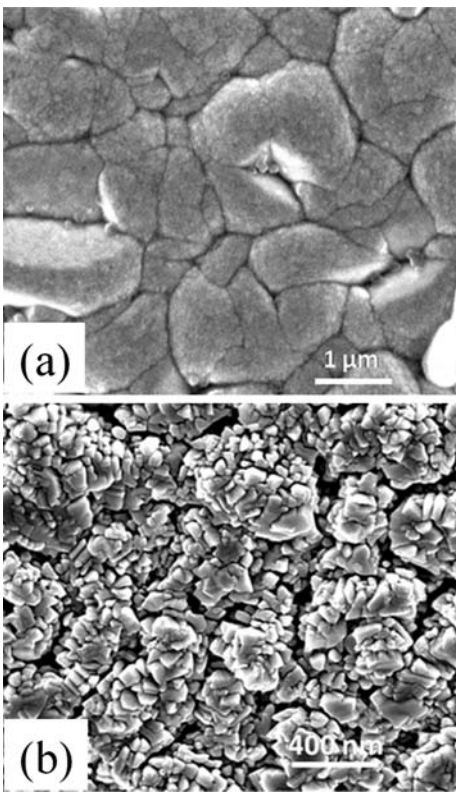

Fig. 4 SEM images of (a) as-sputtered CuO thin film and (b) after the two-step growth process.

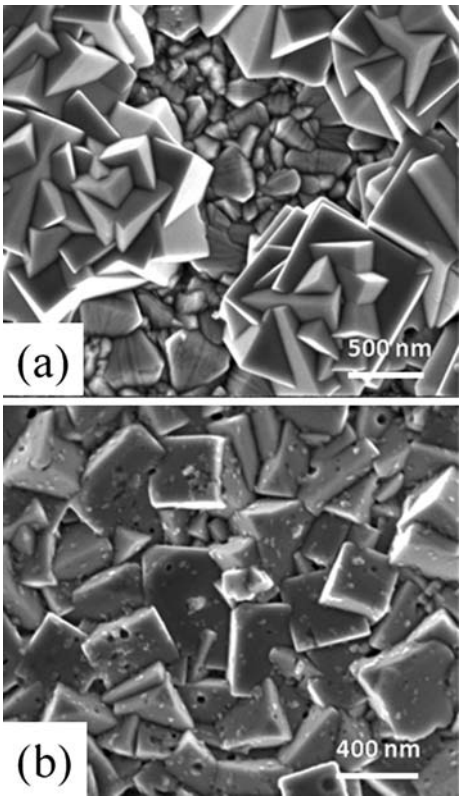

Fig. 5 SEM images of samples deposited using a one-step process at a potential of (a) −0.4 V and (b) −0.5 V.

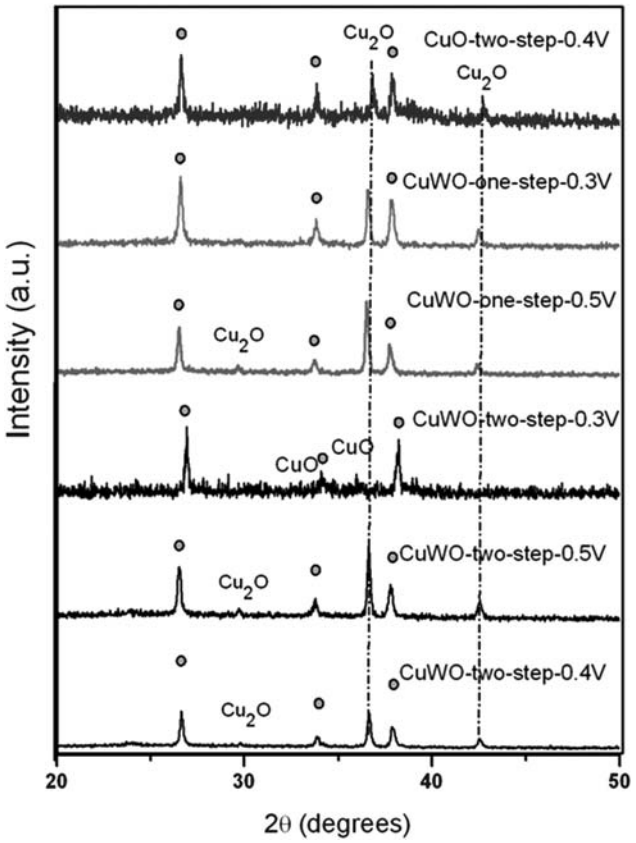

Fig. 6 XRD spectra obtained from samples deposited at different potentials. Peaks labeled as ° are from FTO.

the corrosion of amorphous Cu–W oxide films leads to the special porous structure seen in Fig. 2(b). Without the inclusion of tungsten species, the corrosion of sputtered copper oxide films under positive potential occurred at a much slower pace, but uniformly. Thus, the presence of W in the starting materials is another key factor for the synthesis of copper oxide nanowires using the two-step process.

We have further tried electrochemical deposition using the same pre-sputtered amorphous Cu–W oxide thin film but using only the one-step process, *i.e.*, direct growth without the first corrosion step. Fig. 5(a) and 5(b) show the SEM images of the surface morphology of samples electrochemically deposited using only the one-step process at a potential of −0.4 V and −0.5 V, respectively. It is seen that the one-step growth process can only grow clusters of copper oxide cubes, instead of nanowires.

Fig. 6 shows XRD spectra obtained from the samples electrochemically deposited at different potentials. The sample deposited at a potential of −0.3 V showed very weak XRD intensity, but the CuO peaks were still observed. The other samples showed strong Cu_2O peaks. However, it is difficult to determine in the two-stage samples prepared under −0.4 V and −0.5 V potentials whether the Cu_2O XRD signals are from nanowires or from the underlying cubic crystals.

To confirm the structure and composition concluded from the XRD analysis, the nanowires were examined by TEM and EELS. Fig. 7(a) and 7(b) show TEM images of copper oxide nanowires grown by the two-step process with potentials of −0.4 V and −0.3 V, respectively. We find that the nanowires have a polycrystalline structure. The nanowires grown at a potential of −0.3 V have very small grains that are about 5 to 10 nm in size. This is consistent with the fact that the XRD spectrum obtained from sample CuWO-two-step-0.3V has very weak intensity. Fig. 8 shows the EELS spectra of the Cu L edge in the nanowires from samples CuWO-two-step-0.3V (the lower curve) and CuWO-two-step-0.4V (the upper curve). The EELS data were taken using the nanoprobe electron beam from individual nanowires. The Cu L_2/L_3 peak ratios reveal clearly that the nanowires in sample CuWO-two-step-0.3V are CuO, whereas the nanowires in sample CuWO-two-step-0.4V are Cu_2O, consistent with the results from XRD analysis.

The PEC performance of the samples deposited by the two-step process under chopped light illumination is shown in Fig. 9. All films show cathodic photocurrent, indicating a p-type behavior, and the photocurrent increases with the applied negative potential. The sample deposited at −0.4 V shows the best performance. At a bias of −0.3 V, this sample shows a photocurrent of about −55 μA cm^{-2}, whereas the other two nanowire samples had photocurrents of less than −20 μA cm^{-2}. All samples show high dark currents. Cathodic corrosion of copper oxide could be one of the causes. The inset in Fig. 9 shows the stability test when biased negatively for the sample deposited at −0.4 V at a bias of −0.3 V. It shows good stability under illumination and under negative potential. After an additional 2 h stability test, sample CuWO-two-step-0.4V (Fig. 10) has also shown good stability. The superior stability of copper oxides synthesized by electrodeposition under negative potential is also justified by other studies.[26,27]

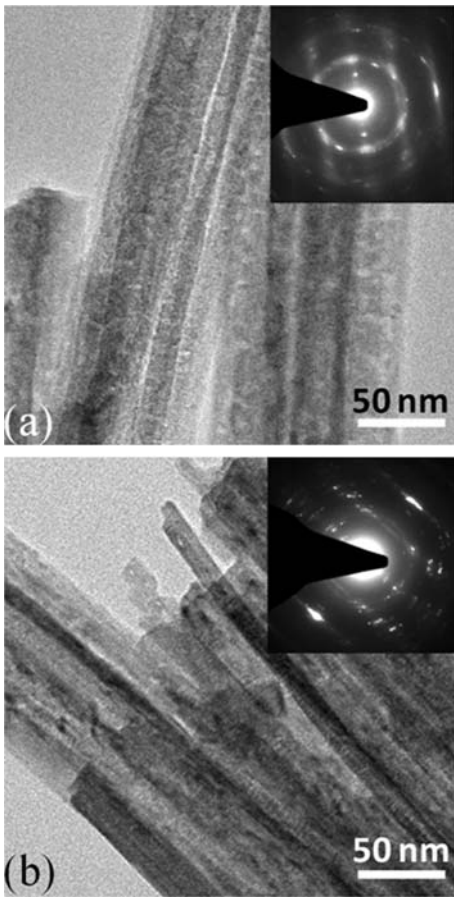

Fig. 7 TEM images of nanowires from (a) sample CuWO-two-step-0.3V and (b) sample CuWO-two-step-0.4V. The insets are corresponding diffraction patterns.

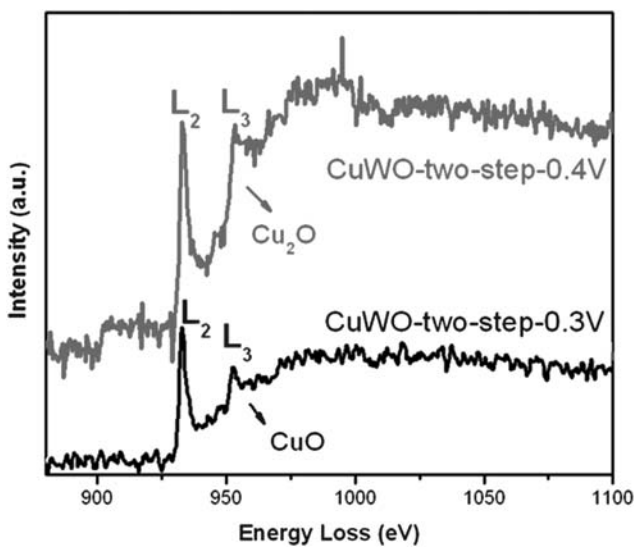

Fig. 8 EELS spectra of Cu L edge in the nanowires of CuWO-two-step-0.3V and CuWO-two-step-0.4V.

The PEC performance of the cube-like samples deposited using the two-step process, but with CuO as the starting material, has also been measured. The polarization curve measured under

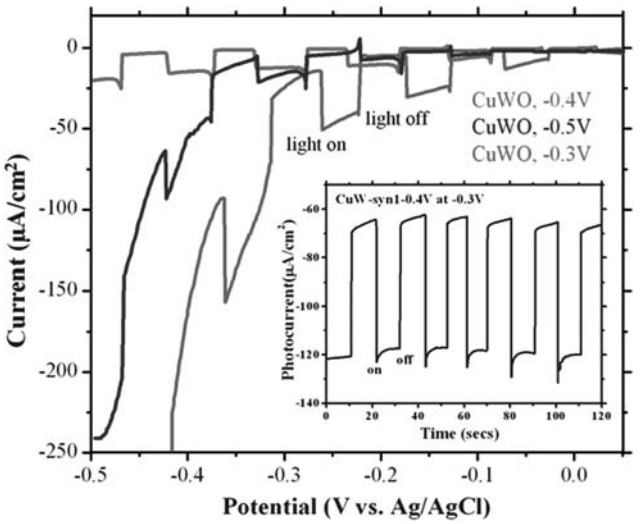

Fig. 9 Polarization curves under chopped light for samples deposited at different potentials. The thermodynamic potential for hydrogen evolution should be at −0.855 V and for oxygen evolution should be at 0.375 V.

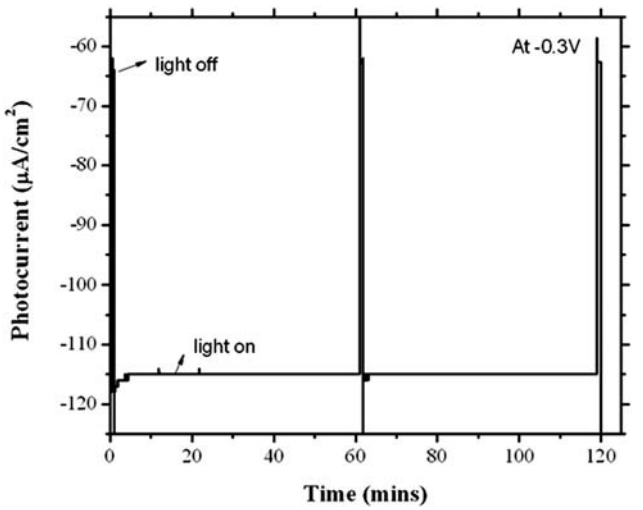

Fig. 10 Stability test of sample CuWO-two-stage-0.4V for 2 h at −0.3 V.

chopped light illumination is shown in Fig. 11. The cube-like Cu_2O also exhibits p-type behavior. However, the photoresponse of the cube-like sample is much lower than the nanowire samples. At −0.3 V, the photocurrent of the cube-like sample is less than −10 μA cm^{-2}.

Moreover, we have characterized the PEC performance of the cube-like samples deposited using the one-step process amorphous Cu–W oxide as the starting material. Fig. 12 shows the polarization curves measured under chopped light illumination. The photoresponse is slightly better for the sample deposited at −0.3 V than that deposited at −0.5 V. However, both photocurrents are less than 10 μA cm^{-2} at −0.3 V. Thus, it is reasonable to conclude that the photocurrent measured from the nanowires samples is contributed mainly by the copper oxide nanowires. The nanowires samples perform much better than the cube-like samples. The higher surface areas and better contact with the

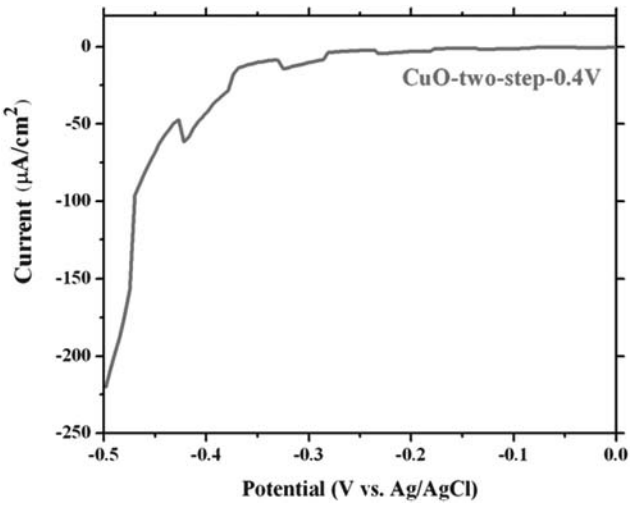

Fig. 11 Polarization curve under chopped light for the sample synthesized by the two-step process, but with CuO as the starting material.

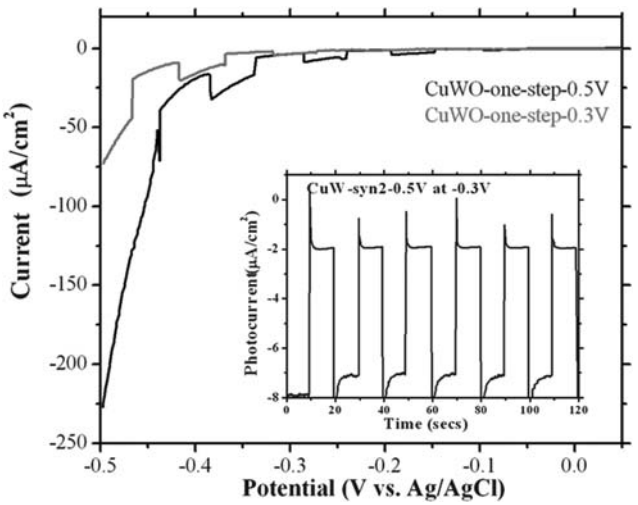

Fig. 12 Polarization curves under chopped light for the samples synthesized by the one-step process, with amorphous Cu–W oxide as the starting materials.

FTO-coated substrates for the nanowires grown by the two-step process could be the reasons for the enhanced performance.

IV. Conclusions

We have synthesized copper oxide nanowires on FTO-coated glass substrates using a two-step growth process. This process enables the growth of copper oxide nanowires without the use of templates and surfactants. We found that the presence of W in the starting materials is critical for copper oxide nanowire formation. The oxidation states, *i.e.*, CuO or Cu_2O, and morphology of nanowires can be controlled by the applied potentials during the second step. Cu_2O nanowires grown using this method at a potential of −0.4 V exhibited the best PEC performance and stability under cathodic bias. Our results suggest that the two-step growth process may be applied to grow other nanostructures for PEC applications. We would like to point out that the utility of these materials for practical water splitting faces many challenges that need to be solved. For example, the valence band edge is too negative to drive the oxygen evolution reaction; the photoconversion efficiency is low even under moderate bias. Finally, others have reported instability of Cu_2O under open-circuit in darkness, which are conditions that practical water-splitting devices will encounter.

Acknowledgements

This work is supported by the U.S. Department of Energy under contract no. DE-AC36-08GO28308.

References

1 G. H. Li, N. M. Dimitrijevic, L. Chen, T. Rajh and K. A. Gray, *J. Phys. Chem. C*, 2008, **112**, 19040–19044.
2 D. Drijvers, H. van Langenhove and M. Beckers, *Water Res.*, 1999, **33**, 1187–1194.
3 T. Ishihara, M. Higuchi, T. Takagi, M. Ito, H. Nishiguchi and T. Takita, *J. Mater. Chem.*, 1998, **8**, 2037–2042.
4 O. Chmaissem, J. D. Jorgensen, S. Short, A. Knizhnik, Y. Eckstein and H. Shaked, *Nature*, 1999, **397**, 45–48.
5 T. Minami, H. Tanaka, T. Shimakawa, T. Miyata and H. Sato, *Jpn. J. Appl. Phys.*, 2004, **43**, L917–L919.
6 S. S. Jeong, A. Mittiga, E. Salza, A. Masci and S. Passerini, *Electrochim. Acta*, 2008, **53**, 2226–2231.
7 Y. S. Chaudhary, A. Agrawal, R. Shrivastav, V. R. Satsangi and S. Dass, *Int. J. Hydrogen Energy*, 2004, **29**, 131–134.
8 F. Marabelli, G. B. Parravicini and F. Salghettidrioli, *Phys. Rev. B: Condens. Matter*, 1995, **52**, 1433–1436.
9 V. T. Agekyan, *Phys. Status Solidi A*, 1977, **43**, 11–42.
10 A. E. Rakhshani, *Solid-State Electron.*, 1986, **29**, 7–17.
11 J. F. Pierson, A. Thobor-Keck and A. Billard, *Appl. Surf. Sci.*, 2003, **210**, 359–367.
12 L. S. Huang, S. G. Yang, T. Li, B. X. Gu, Y. W. Du, Y. N. Lu and S. Z. Shi, *J. Cryst. Growth*, 2004, **260**, 130–135.
13 N. Ozer and F. Tepehan, *Sol. Energy Mater. Sol. Cells*, 1993, **30**, 13–26.
14 R. V. Kumar, Y. Mastai, Y. Diamant and A. Gedanken, *J. Mater. Chem.*, 2001, **11**, 1209–1213.
15 S. Deki, K. Akamatsu, T. Yano, M. Mizuhata and A. Kajinami, *J. Mater. Chem.*, 1998, **8**, 1865–1868.
16 A. P. Chatterjee, A. K. Mukhopadhyay, A. K. Chakraborty, R. N. Sasmal and S. K. Lahiri, *Mater. Lett.*, 1991, **11**, 358–362.
17 T. Mahalingam, J. S. P. Chitra, S. Rajendran, M. Jayachandran and M. J. Chockalingam, *J. Cryst. Growth*, 2000, **216**, 304–310.
18 X. M. Liu and Y. C. Zhou, *Appl. Phys. A: Mater. Sci. Process.*, 2005, **81**, 685–689.
19 L. C. Wang, N. R. de Tacconi, C. R. Chenthamarakshan, K. Rajeshwar and M. Tao, *Thin Solid Films*, 2007, **515**, 3090–3095.
20 A. E. Rakhshani and F. K. Barakat, *Mater. Lett.*, 1987, **6**, 37–40.
21 T. D. Golden, M. G. Shumsky, Y. C. Zhou, R. A. VanderWerf, R. A. VanLeeuwen and J. A. Switzer, *Chem. Mat.*, 1996, **8**, 2499–2504.
22 K. S. Ahn, S. Shet, T. Deutsch, C. S. Jiang, Y. F. Yan, M. Al-Jassim and J. Turner, *J. Power Sources*, 2008, **176**, 387–392.
23 K. S. Ahn, Y. Yan, S. Shet, K. Jones, T. Deutsch, J. Turner and M. Al-Jassim, *Appl. Phys. Lett.*, 2008, **93**, 3.
24 L. Chen, S. Shet, H. Tang, K. S. Ahn, T. Deutsch, H. Wang, Y. Yan, J. Turner and M. Al-Jassim, 2010, in preparation.
25 K. S. Ahn, Y. F. Yan, S. H. Lee, T. Deutsch, J. Turner, C. E. Tracy, C. L. Perkins and M. Al-Jassim, *J. Electrochem. Soc.*, 2007, **154**, B956–B959.
26 C. C. Hu, J. N. Nian and H. Teng, *Sol. Energy Mater. Sol. Cells*, 2008, **92**, 1071–1076.
27 P. E. de Jongh, D. Vanmaekelbergh and J. J. Kelly, *Chem. Commun.*, 1999, 1069–1070.